ISSN 2072-5981
doi: 10.26907/mrsej

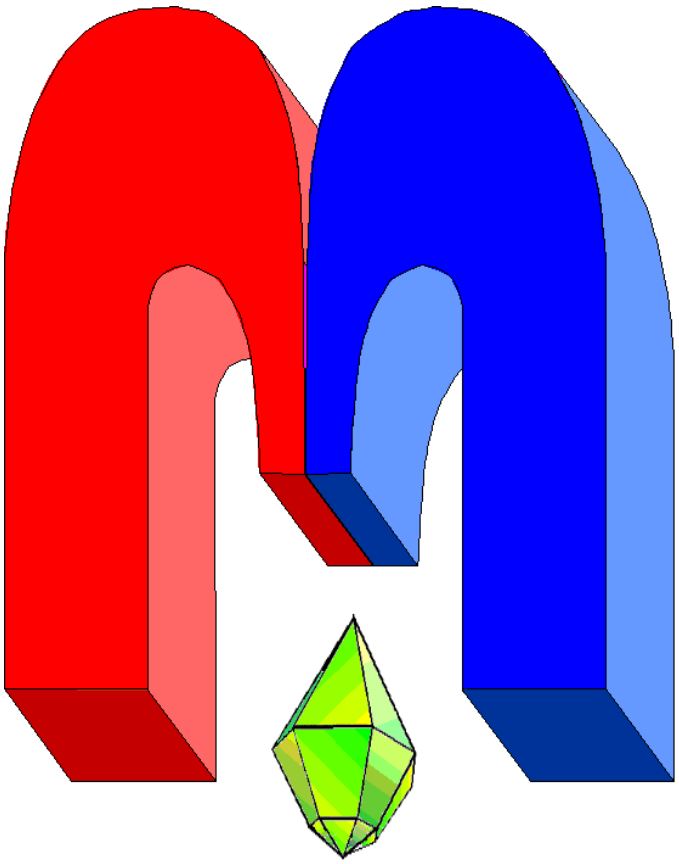

Magnetic Resonance in Solids

Electronic Journal

Volume 22
Issue 2
Article No ***20201***
1-11 pages
2020
doi: **10.26907/mrsej-20201**

http://mrsej.kpfu.ru
http://mrsej.ksu.ru

Established and published by Kazan University
Endorsed by International Society of Magnetic Resonance (ISMAR)
Registered by Russian Federation Committee on Press (#015140),
August 2, 1996
First Issue appeared on July 25, 1997

"***Magnetic Resonance in Solids. Electronic Journal***" (**MRS*ej***) is a peer-reviewed, all electronic journal, publishing articles which meet the highest standards of scientific quality in the field of basic research of a magnetic resonance in solids and related phenomena.

Indexed and abstracted by
Web of Science (*ESCI*, Clarivate Analytics, from 2015), *Scopus* (Elsevier, from 2012), *RusIndexSC* (*eLibrary*, from 2006), *Google Scholar*, *DOAJ*, *ROAD*, *CyberLeninka* (from 2006), *SCImago Journal & Country Rank*, etc.

Technical Editor
Maxim **Avdeev** (KFU, Kazan)

* In Kazan University the Electron Paramagnetic Resonance (EPR) was discovered by Zavoisky E.K. in 1944.

Spin relaxation of the $^{171}Yb^{3+}$ ion in the $Y_2{}^{28}SiO_5$ crystal

R.F. Likerov[1,*], V.F. Tarasov[1], A.A. Sukhanov[1], A.V. Shestakov[1], R.M. Eremina[1], Yu.D. Zavartsev[2], S.A. Kutovoi[2]

[1]Zavoisky Physical-Technical Institute, Federal Research Center "Kazan Scientific Center of RAS", Sibirsky tract, 10/7, Kazan, 420029, Russia

[2]Prokhorov General Physics Institute, Russian Academy of Sciences, Vavilova St., 38, Moscow, 119991, Russia

[*]*E-mail: rodionlikerov@gmail.com*

(Received December 3, 2019; revised May 3, 2020; accepted May 14, 2020; published May 18, 2020)

Pulse methods of electron paramagnetic resonance (EPR) are used to measure relaxation behavior and crystal environment of ^{171}Yb impurity ions in a single crystal of yttrium orthosilicate (Y_2SiO_5) grown with an isotopically pure ^{28}Si with a zero value of the nuclear spin. It is shown that for an ytterbium ion substituting an yttrium ion in a six-fold oxygen environment, the spin-lattice relaxation time is approximately an order of magnitude greater than that for the ytterbium ion substituting an yttrium ion in a seven-fold oxygen environment. Measurements of the phase relaxation times by two-pulse Hahn echo and Carr-Purcell-Meiboom-Gill (CPMG) multiple pulse sequence revealed strong influence of spectral diffusion on the time of phase relaxation at temperatures less than 9 K. Two magnetically different ytterbium paramagnetic centers were definitely attributed to two structurally different ytterbium positions in the Y_2SiO_5 crystal lattice relative by the electron spin echo envelope modulation (ESEEM) method. Based on the data obtained, the most probable location of the $^{171}Yb^{3+}$ ion in the Y_2SiO_5 crystal lattice was determined.

PACS: 71.70.Ch, 76.10.Dg, 76.30.Kg

Keywords: orthosilicate crystals, EPR, optical materials, ytterbium ion, spin-spin relaxation time, spin-lattice relaxation time

1. Introduction

In the last few decades, dielectric crystals doped with rare-earth ions have been studied intensively. These crystals are considered as promising materials for solid-state quantum processing and quantum communication devices. Also, it is possible to use these crystals as possible candidates for a coherent interface between optical and microwave photons. Paramagnetic centers formed in the crystals by the impurity rare-earth ions are considered a suitable basis in quantum memory applications (see ref. [1–5]). For quantum memory realization it is preferable to use rare-earth isotopes with non-zero nuclear spins because they can be used for storing quantum states. Currently, there are available a lot of different crystal hosts, which can be used in quantum applications. Among these are orthosilicates, which are already used in various areas. Yttrium orthosilicate Y_2SiO_5 (YSO) single crystals doped with rare-earth ions are actively used for microlasers and diode-pumped solid-state lasers [6, 7]. Earlier studies of the structure of YSO were conducted in late 60s by Michel et al. [8] and Maksimov et al. [9, 10], which were later revised by Becerro et al. and Persson et al. [11, 12]. Recently, a few articles on the study of doped rare-earth ions in YSO crystals have been published, e.g. neodymium [3], erbium [13], thulium [4], europium [14], praseodymium [15] and ytterbium [16].

There are two isotopes of ytterbium Yb^{3+} with non-zero nuclear spins, of which $^{171}Yb^{3+}$ has the smallest nuclear spin $I = 1/2$, which yields the simplest energy level diagram for the ground and excited states. The impurity ytterbium ions replace yttrium in one of two structurally

nonequivalent positions with the point symmetry group C_1, denoted by Y1 and Y2 [9,10]. They form two magnetically inequivalent centers whose principal magnetic axes are mirror-symmetric with respect to the (ac) plane. These centers become equivalent if the external magnetic field is parallel to the crystallographic b-axis or lies in the (ac) plane. The Stark energy levels of the Yb^{3+} ion in Y_2SiO_5 were identified in [17,18]. Studies of the polarization and relative intensities of transitions between the sublevels $^2F_{7/2}$ and $^2F_{5/2}$ in Yb^{3+}:Y_2SiO_5 crystals, where Yb^{3+} ions occupy the positions with C_1 point symmetry, have been performed and presented by Welinski et al. [2]. It should be noted that in contrast to the results of Maksimov [9,10], where yttrium ions with a six-oxygen environment has label Y1, according to [19] this position is designated as site 2. Whereas in the notation of Maximov [9,10], yttrium ions with a seven-oxygen environment were denoted as Y2, in [19] this position is designated as site 1. The principal values of the g-matrix for ytterbium ions in orthosilicate were determined by Tiranov et al. [19] to be: $g_x = 0.31$, $g_y = 1.60$, $g_z = 6.53$ for site 1 and $g_x = 0.13$, $g_y = 1.50$, $g_z = 6.06$ for site 2. The principal values of the hyperfine interaction A-matrix (expressed in GHz) were determined [19] to be: $A_x = 0.481$, $A_y = 1.159$, $A_z = 5.251$ and $A_x = 0.126$, $A_y = 1.184$, $A_z = 4.867$ for sites 1 and 2, respectively.

The temperature dependencies of the spin-lattice relaxation time for the ytterbium ions doped in yttrium orthosilicate were published in the papers [16, 20]. It turned out that the absolute value of the spin-lattice relaxation time at 5K obtained by both groups differs by one orders of magnitude. In this regard, we have measured the temperature dependence of the spin-lattice relaxation time for the ytterbium ions doped in yttrium orthosilicate.

As noted earlier, for quantum memory applications the rare-earth ions with non-zero nuclear spins are preferable over the ions with zero nuclear spin. Use of only one isotope helps to achieve high optical density of the resonant environment for low concentration of impurity ions. There are two choices for ytterbium: to use only $^{171}Yb^{3+}$ or $^{173}Yb^{3+}$ ion isotopes. Presence of other isotopes is undesirable since they reduce the phase memory time of the active ions due to the spin-spin interactions. In addition to using a monoisotopic impurity, the host crystal Y_2SiO_5 can be modified by using the ^{28}Si isotope instead of the Si with natural isotope abundance. This will reduce inhomogeneous and homogeneous broadening of the resonance lines of the impurity ions.

In this paper we present the results of the pulsed electron paramagnetic resonance measurements for $Y_2{}^{28}SiO_5$ doped with 0.001 % ytterbium ions. We measured the spin-lattice relaxation times and spin-spin relaxation times (also known as phase memory time or coherence time) and their temperature dependencies. Electron spin echo envelope modulation (ESEEM) spectroscopy has proven to be a very useful technique for studying unresolved hyperfine interactions (HFI). ESEEM has been employed to characterize the local environment of complexes with paramagnetic ions. Solving the inverse problem in a ESEEM experiment in complex systems often becomes a challenge due to overlapping signals from different sources. In our previous publications [21, 22], we showed that the analysis of the rescaled ESEEM data recorded at several resonance transitions of the Nd^{3+} ion doped in YSO crystal allows one to characterize the spin-spin interactions of a large number of neighboring magnetic nuclei. This makes it possible to study the local environment of the ion and, as a consequence, the distortions caused by the doped ion. The rescaling method is applied here to study the local structure of a crystal doped by Yb^{3+} ions.

2. Materials and methods

2.1. Y_2SiO_5 crystal

According to Maksimov [9] in YSO crystal there are two structurally non-equivalent yttrium sites: the Y1 site in which the yttrium is surrounded by six oxygen atoms and Y2 site in which the yttrium is surrounded by seven oxygen atoms. For impurity ions substituting Y ions in these sites there are two magnetically non-equivalent centers. These magnetically non-equivalent centers are resulting in different behavior of the paramagnetic centers in the magnetic field. The Y_2SiO_5 crystal belongs to the $C^6{}_{2h}$ (Schoenflies notation)/ $I_{2/a}$ (Hermann-Mauguin notation) space group [9] with the following unit cell parameters: $a = 10.410 \pm 0.003$ Å, $b = 6.721 \pm 0.002$ Å, $c = 12.490 \pm 0.005$ Å. Structure of the yttrium centers in the Y_2SiO_5 crystal is shown at Fig. 1.

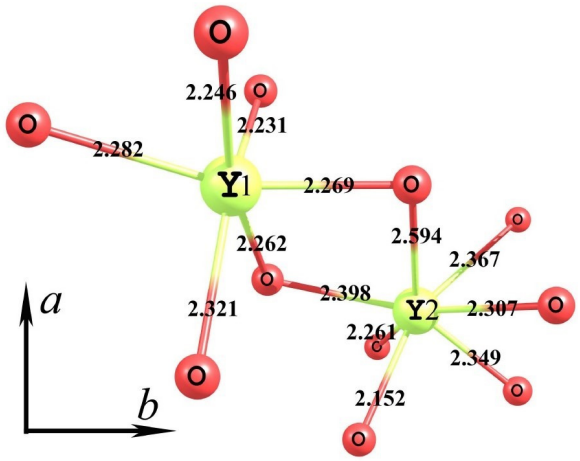

Figure 1. Structure of the yttrium centers in the Y_2SiO_5 crystal [23].

The ytterbium-doped $Y_2{}^{28}SiO_5$ crystal was grown by the Czochralski method in Ir crucibles in the 99 vol.% Ar + 1 vol.% O_2 atmosphere. The purity of the primary components, e.g. $^{28}SiO_2$, Y_2O_3 and $^{171}Yb_2O_3$ was no worse than 99.75 %. After the growing process, 0.001% $^{171}Yb^{3+}$:$Y_2{}^{28}SiO_5$ crystal was investigated by X-ray diffraction analysis in order to find the directions of main crystallographic axes (a, b, c), $\alpha = 102°$. For pulsed EPR measurements the crystal was cut along the D_1, D_2, b main axes, the dimensions of the samples are $2 \times 2 \times 5\,\mathrm{mm}^3$ (D_1, b, D_2).

2.2. Experimental technique

EPR is a convenient method for studying paramagnetic centers. By obtaining and fitting EPR data the values of the g and the A matrixs can be estimated. The pulsed EPR method is used to measure the spin-lattice and the spin-spin relaxation times and their temperature dependencies. The pulsed EPR experiments were carried out with the X - band Bruker ELEXYS E680 spectrometer. This spectrometer is equipped with a helium flow cryostat, which allows to take measurements in the temperature range from 4 to 300 K.

3. Results and Discussion

3.1. Echo-detected spectroscopy

Echo-detected spectrum for ^{171}Yb:$Y_2{}^{28}SiO_5$ is shown at Fig. 2. Two groups of hyperfine structure lines are observed in this spectrum, each of the group is corresponding to ytterbium sites 1

or 2. Orientations of the principal axes of the g-matrix for the Yb^{3+} ions in the two crystallographic sites (site 1 and site 2) were presented in [19]. The magnetic properties of the ytterbium ions in YSO are quasi-one dimensional (g_z much more than g_x, g_y), but the orientations of the z-axes are different for sites 1 and 2. In [19] the Euler angles are presented for the g-matrixs of the ytterbium ion for the two sites. In the notation used, β is the angle between z-axis of the g-matrix and the crystallographic axis b. The values of β for $^{171}Yb^{3+}$ ions in site 1 and site 2 are $\beta = 88.7°$ and $\beta = 11.8°$, respectively.

There are two magnetically nonequivalent magnetic centers for both structurally nonequivalent sites of the impurity ytterbium ions. Magnetic properties of magnetically nonequivalent centers are connected by mirror plane (ac). Therefore, if the external magnetic field is parallel to the b-axis EPR spectra of the two magnetically nonequivalent centers coincide. There is slight misalignment on between directions of magnetic field and b-axis in our case. This misalignment results in splitting of the EPR spectra belonging to the magnetically nonequivalent centers. This splitting is due to different values of projections of magnetic field on the b-axis and depends dramatically on the angle β between the z-axis of paramagnetic center and the orientation of the magnetic field. For the Yb^{3+} ion at site 1 the z-axis is almost perpendicular to the magnetic field ($\beta = \pm 88.7°$). Then change of projection of the magnetic field on the z-axis, and consequently shift of EPR lines positions on the spectrum is proportional to $\sin(\varphi)$. For the Yb^{3+} ion at site 2 orientations of the z-axis are close to the direction of the magnetic field ($\beta = \pm 11.8°$). Then change of projection of the magnetic field on the z-axis, and consequently shift of EPR lines positions on the spectrum is proportional to $\sqrt{1 - \sin^2(\varphi)}$. As a result at small values of φ the splitting between lines of two magnetically nonequivalent centers of the site 1 is much more than it is for the site 2.

For this reason, only two lines of the of the hyperfine structure (HFS) are observed in the spectrum for the $^{171}Yb^{3+}$ ion at site 2, shown on left in Fig. 2. Four lines are observed in the spectrum for the $^{171}Yb^{3+}$ ion at site 1, shown on right in Fig. 2. The low-intensity line between two more intense HFS lines of the $^{171}Yb^{3+}$ ion at site 2 is due to the presence of the even ytterbium isotopes with zero nuclear spin, being inadvertently present in crystal during the growth process. The spin-lattice and the spin-spin relaxation times for the $^{171}Yb^{3+}$ isotope were measured for the resonance lines occurring at the fields $B_0 = 1050\,\mathrm{mT}$ for site 1 and $B_0 = 88\,\mathrm{mT}$ for site 2.

3.2. Spin-lattice relaxation

The spin-lattice relaxation times were measured by the echo saturation method with the fast repetition time of the two pulse sequence $(\pi/2)_x(16\,\mathrm{ns}) - \tau - (\pi)_x(32\,\mathrm{ns})$ in the temperature range from 5 to 7 K, and by the inversion recovery method above 8 K where the pulse sequence was $(\pi)_x(32\,\mathrm{ns}) - T - (\pi/2)_x(16\,\mathrm{ns}) - \tau - \pi - \tau$, the T time was changed with $\tau = 200\,\mathrm{ns}$. After the measurements, the experimental dependencies of the echo intensity were fitted and the values of the T_1 were estimated. The spin-lattice relaxation time dependencies on the temperature are shown in Fig. 3.

Expression (1) was used from Abragam and Bleaney [24]:

$$T_1^{-1} = C_\mathrm{D} T + C_\mathrm{R} T^9 + C_\mathrm{O} e^{-\Delta/kT}, \tag{1}$$

where the first term is due to one-phonon process when the phonon frequency is equal to the frequency of the EPR transition, the second term is due to the Raman two-phonon process and the third term is due to the two-phonon Orbach-Aminov [25] relaxation process. The

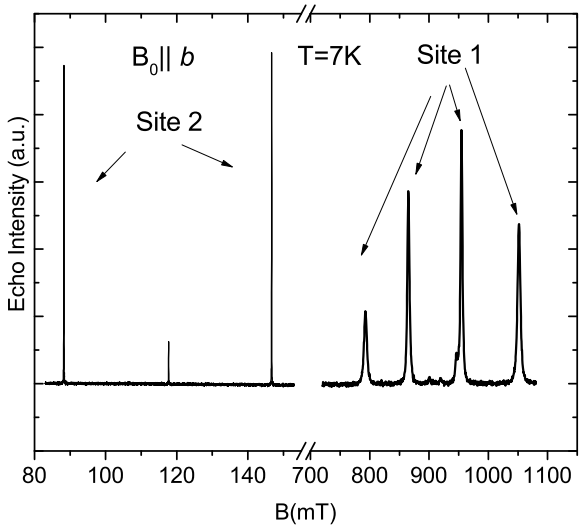

Figure 2. Echo-detected spectrum for $Y_2{}^{28}SiO_5$:$^{171}Yb^{3+}$ (0.001% at.) at 7 K and at the microwave frequency $\nu \approx 9.81$ GHz.

Orbach-Aminov process has little effect on the spin-lattice relaxation of Yb^{3+} ions below 10 K. Energy gap Δ between ground and first excited states of $^2F_{7/2}$ are taken from Stark energy level structure, see Tab. 1.

Table 1. Electron energy levels of Yb^{3+} ion in Y_2SiO_5

	Site 1	Site 2
ε_0 (cm^{-1})	0	0
ε_1(cm^{-1})	113	236
ε_2(cm^{-1})	494	615
ε_3(cm^{-1})	715	964

Fitting parameters C_D, C_R, C_O for the spin-lattice relaxation times are presented in Table 2.

Table 2. Fitting parameters of the spin-lattice relaxation times for the $^{171}Yb^{3+}$ ion in the $Y_2{}^{28}SiO_5$ crystal

Parameter	Site 1	Site 2	Yb^{3+}, Site 1 [20]	Yb^{3+}, Site 2 [20]
C_D [$s^{-1}K^{-1}$]	0.004	0.005	17.4	5.4
C_R [$s^{-1}K^{-n}$]	$(3.1 \pm 0.1)\cdot10^{-5}$	$(1.7 \pm 0.1)\cdot10^{-6}$	$3\cdot10^{-5}$	$2.5\cdot10^{-5}$
C_O [s^{-1}]	$(8.2\pm0.1)\cdot10^{9}$	-	$9\cdot10^{11}$	$10\cdot10^{9}$
Δ [K]	162.6	-	107	97
Δ [cm^{-1}]	113	-	74	67

Comparing the obtained time of spin-lattice relaxation at 5 K (1 s) in our experiment for the ytterbium ions doped in an isotopically pure crystal $Y_2{}^{28}SiO_5$ for site 2 with one from the paper [16] (0.025 s at 5 K) and from paper [20] (0.1 s) demonstrates that the spin-lattice relaxation times for the spins of ytterbium ions doped in an isotopically pure crystal $Y_2{}^{28}SiO_5$ is the one order longer than in the crystal with a natural abundance of silicon ion Y_2SiO_5.

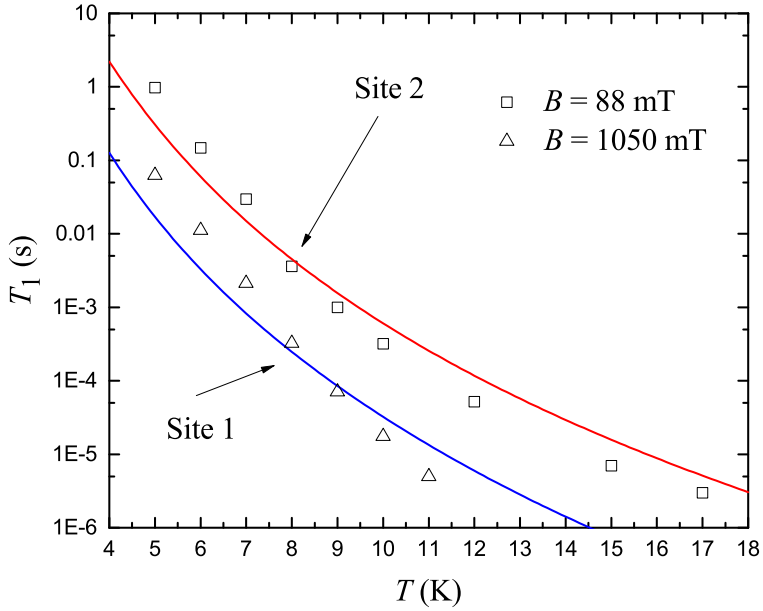

Figure 3. Temperature dependencies of the spin-lattice relaxation times in the $Y_2{}^{28}SiO_5$:$^{171}Yb^{3+}$ (0.001% at.) for two crystallographic sites at the microwave frequency $\nu \approx 9.8$ GHz. Solid lines are a fitting by the expression 1 with the parameters presented in Tab. 2. Blue line is for Site 1 and red line is for Site 2.

3.3. Spin-spin relaxation

In order to estimate the perspective of making the quantum memory on electron spins, it is necessary to obtain the coherence times, which for electron spins are equal to phase relaxation times. In many cases, significant reduction of the coherence time is due to spectral diffusion. This process is responsible for varying precession frequency of the spins with orientations of the neighbor electron and nuclear spins are changed randomly. This leads to dephasing of magnetization vectors of different spin groups [26]. Spin-spin relaxation times measurements were done by primary echo decay method and Carr-Purcell-Meiboom-Gill (CPMG) method. The pulse sequence for primary echo decay is $(\pi/2)_x(16\,\text{ns}) - \tau - (\pi)_x(32\,\text{ns}) - \tau -$ echo. The interpulse delay τ was changed with the 200 ns step, which allows to obtain the dependencies of the echo intensity on the time of interpulse delay. The measurements were done in the temperature range from 5 to 12 K. Experimental data was fitted by exponential decay: $I = I_0 + I_1 \cdot \exp(-2\tau/T_2)$, where I is intensity, I_0 is white noise, 2τ is time, T_2 is spin-spin relaxation time. The T_2 values, obtained at the different temperatures, represents the temperature dependence of the spin-spin relaxation times. This dependence is shown in Fig. 4 (black square markers).

There is a strong influence of the spectral diffusion to the relaxation time values in the primary echo decay method. In order to suppress the spin diffusion processes we used the Carr-Purcell-Meiboom-Gill method [27]. The CPMG experiment was carried out using the pulse sequence $(\pi/2)_x - [\tau(5\,\mu\text{s}) - (\pi)_y - \tau(5\,\mu\text{s}) - \text{echo}]_{N=32}$ with the durations of the $\pi/2$-pulse and π-pulse being 16 ns and 32 ns, respectively. This allowed us to obtain time values seven times longer than from the primary echo decay experiment, resulting $T_2 \approx 146 \pm 10\,\mu$s at $T = 5$ K. The spin-spin relaxation times temperature dependencies from the CPMG experiment are shown at Fig. 4 (red circle markers).

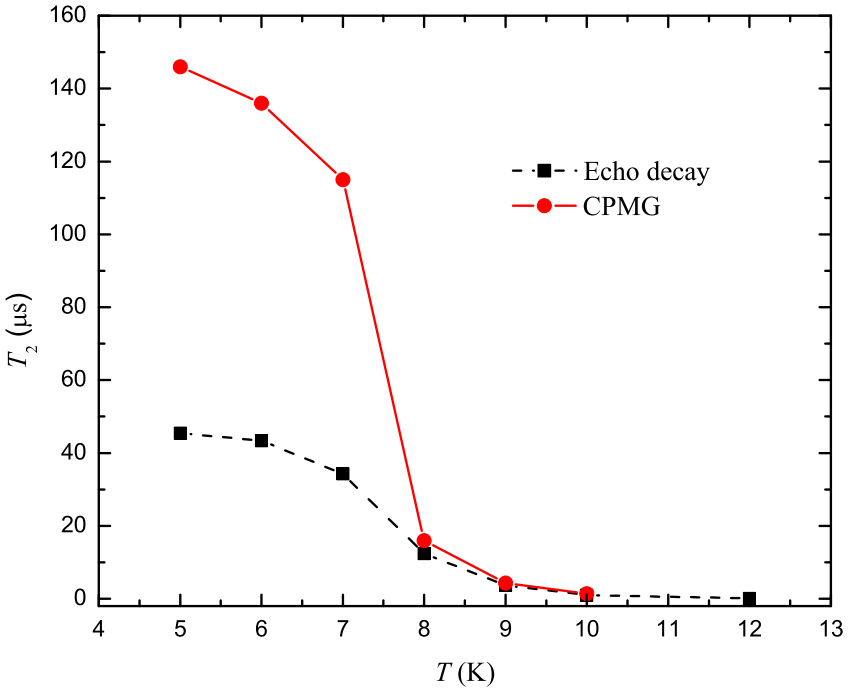

Figure 4. Temperature dependencies of the spin-spin relaxation times in the in the $Y_2{}^{28}SiO_5{:}^{171}Yb^{3+}$ (0.001 % at.), obtained by the echo decay and the CPMG sequences at the microwave frequency $\nu \approx 9.8$ GHz.

3.4. Electron spin echo envelope modulation

The ESEEM data were recorded using a three-pulse stimulated echo pulse sequence with a 16 ns $\pi/2$-pulse. The experiments on the YSO crystal were performed at 8 K with the crystal aligned such the external magnetic field was parallel the b-axis. In this case two different crystallographic sites have different effective g-factor. ESEEM measurements were carriied out for both resonance lines corresponding to site 2 in Fig. 2. It has been shown previously [21] that the analysis of the 2D ESEEM data becomes straightforward in by the use of the parameter (the rescaled representation):

$$F = \Omega^2 - \omega^2. \tag{2}$$

Here, Ω refers to the frequency observed in the ESEEM experiment, and ω is the yttrium nuclear Larmor frequency. The ESEEM data interpreted according to this procedure are shown in Fig. 5 for two yttrium nuclear Larmor frequencies for two different magnetic fields. It has been shown [21,22], that for $I = 1/2$ the required frequencies, F are given by:

$$F^{\pm} = \omega^2 \pm A\omega + (A^2 + B^2)/4, \tag{3}$$

where A and B are the hyperfine interaction (HFI) parameter, describing the hyperfine Hamiltonian as:

$$H_{\mathrm{HFI}} = S_z(AI_z + BI_x). \tag{4}$$

For the detailed description of the rescaling procedure see [21, 22]. Fermi-contact interaction can't give a ESEEM signal. This was first shown in paper [28]. The HFI from a remote nucleus is determined by the dipole-dipole interaction between the electron and nuclear spins, so that the parameters A and B are described as:

$$A = \omega_{\mathrm{dd}}(1 - 3\cos^2\theta), \tag{5}$$

$$B = \frac{3}{2}\omega_{\mathrm{dd}}\sin(2\theta). \tag{6}$$

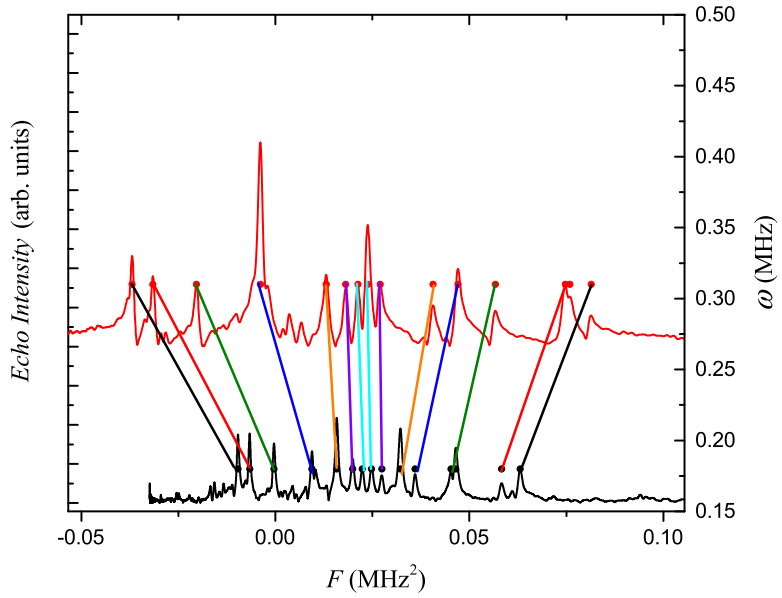

Figure 5. ESEEM data rescaled according to the procedure described in the text (the equations 3-7). Each pair of lines represent the functions $F^{\pm}$ with the particular set of HFI parameters for each Y nucleus in close vicinity to Y1 position occupied by Yb^{3+} ion.

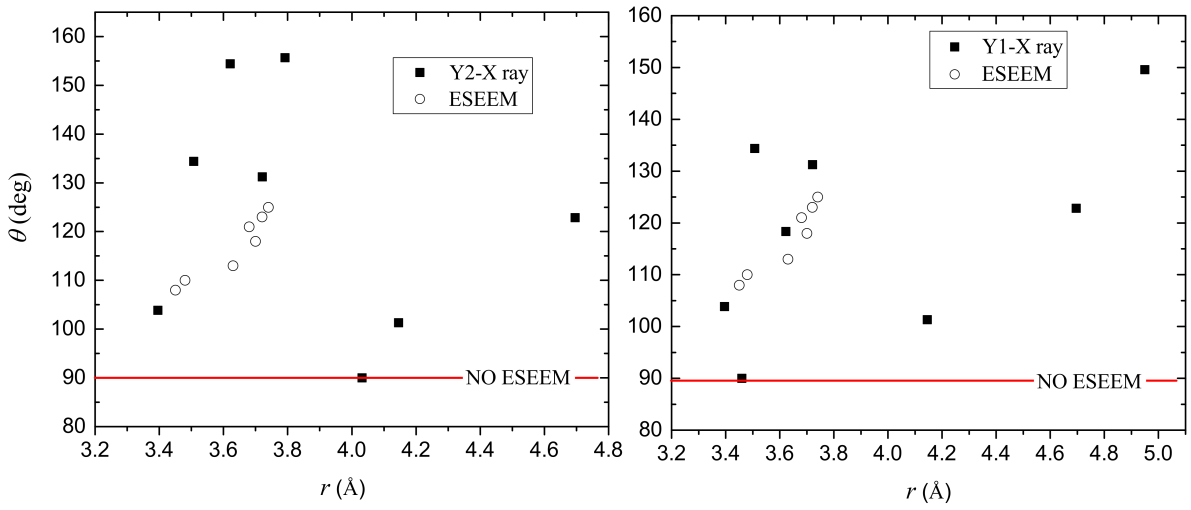

Figure 6. The comparison of the parameters obtained from ESEEM spectroscopy and X-ray crystallography for the two yttrium sites

Here, θ is an angle between the direction of the electron spin magnetic moment and the radius-vector $\mathbf{r}$ connecting the electron and nuclear spins. The frequency of the dipole-dipole interaction $\omega_{\rm dd}$ is given by:

$$\omega_{\rm dd} = \frac{\omega_0}{4\pi}\frac{\mu_{\rm e}\mu_{\rm n}}{\hbar}\frac{g_{\rm e}g_{\rm n}}{r^3}, \tag{7}$$

where $\mu_{\rm e}$, $\mu_{\rm n}$ are electron and nuclear magnetons, $g_{\rm e}$, $g_{\rm n}$ are effective electron and nuclear g-factors. There are two solutions for the variables $\mathbf{r}$ (r_1 and r_2, see the Table 3) and θ (θ_1 and θ_2, see the Table 3) for each set of values of the magnitudes of A and B. The corresponding solutions are listed in Table 3.

The data in Fig. 5 are fitted to the equations (3-7) and are presented by the pairs of lines with the same color. The best-fit parameters are listed in Table 3.

Table 3. Fitting parameters of the ESEEM data and X-ray data for the $^{171}Yb^{3+}$ ion in the $Y_2{}^{28}SiO_5$ crystal

Parameter	1	2	3	4	5	6	7
A [MHz]	0.2	0.18	0.13	0.08	0.039	0.018	0.008
B [MHz]	0.25	0.26	0.26	0.28	0.31	0.31	0.31
r_1 [Å] ESEEM	3.45	3.48	3.63	3.7	3.68	3.72	3.74
θ_1 [deg] ESEEM	108	110	113	118	121	123	125
r_2 [Å] ESEEM	3.99	3.98	4.03	3.95	3.79	3.77	3.76
θ_2 [deg] ESEEM	33	36	40	46	51	53	54
r [Å] Y2-X ray	3.3953	3.5069	3.6208	3.7212	3.7915	4.0314	4.1455
θ [deg] Y2-X ray	103.86	134.39	154.44	131.24	155.66	90	101.31
r [Å] Y1-X ray	3.3953	3.4593	3.5069	3.6227	3.7212	4.1455	4.6955
θ [deg] Y1-X ray	103.86	90	134.39	118.36	131.24	101.316	122.85

The comparison of the parameters obtained from ESEEM spectroscopy and X-ray crystallography [9] data sets for the two crystallographic positions of yttrium atoms is presented in Fig. 6. We have studied the mutual distances assuming that the ESEEM signal is detected from impurity ions located at site Y1 or site Y2 (Fig. 6). The estimated distances from ESEEM data are better correlated with the data from X-ray diffraction crystallography for the Yb^{3+} ion in Y1 position in the Maksimov notations [9] and site 2 according [19]. We verified that the impurity Yb^{3+} ion, labeled as site 1, does indeed occupies occupy the crystallography site Y1 with a six-oxygen environment.

4. Conclusions

A single crystal of yttrium orthosilicate ($Y_2{}^{28}SiO_5$) doped with $^{171}Yb^{3+}$ monoisotopic ions was studied by pulsed X-band EPR. The temperature dependencies of the spin-lattice relaxation times of two paramagnetic centers formed by ytterbium ions replacing yttrium ions at different crystal positions are measured. It is established that the spin-lattice relaxation times for the spins of ytterbium ions doped in an isotopically pure crystal $Y_2{}^{28}SiO_5$ (site 2) is the one order longer than in the crystal with a natural abundance of silicon ion Y_2SiO_5.

Measurements of temperature dependencies of the phase relaxation time of electron spins using a two-pulse Hahn echo and multi-pulse CPMG sequence showed that at temperatures below 9 K, the memory coherence time of electron spins is mainly determined by spectral diffusion. At 5 K, application of the CPMG pulse sequence enlarges the phase relaxation time by about 3.2 times from 46 μs as measured by the two-pulse Hahn echo up to up to 147 μs. The spatial location of two magnetically different Yb^{3+} ions substituting two structurally different Y^{3+} ions was definitely determined by comparative analysis of ESEEM spectra of different hyperfine components of the $^{171}Yb^{3+}$ spectrum.

Acknowledgments

This work was supported by the Russian Science Foundation (project no. 16-12-00041).

References

1. Thiel C. W., Böttger T., Cone R. L. *Journal of Luminescence* **131**, 353 (2011)

2. Welinski S., Ferrier A., Afzelius M., Goldner P. *Phys. Rev. B* **94**, 155116 (2016)

3. Sukhanov A. A., Tarasov V. F., Eremina R. M., Yatsyk I. V., Likerov R. F., Shestakov A. V., Zavartsev Y. D., Zagumennyi A. I., Kutovoi S. A. *Applied Magnetic Resonance* **48**, 589 (2017)

4. Sukhanov A. A., Tarasov V. F., Zavartsev Y. D., Zagumennyi A. I., Kutovoi S. A. *JETP Letters* **108**, 210 (2018)

5. Morton J. J. L., Bertet P. *J. Magn. Res.* **287**, 128 (2018)

6. Rakov N., Maciel G. S. *Journal of the American Ceramic Society* **103**, 1782 (2020)

7. Li Y. L., Jiang H. L., Ni T. Y., Zhang T. Y., Tao Z. H., Zeng Y. H. *Laser Physics* **21**, 670 (2011)

8. Michel C., Buisson G., Bertaut E. *Comptes rendus hebdomadaires des seances de l academie des sciences serie B* **264**, 397 (1967)

9. Maksimov B. A., Kharitonov Y. A., Ilyhin V. V., Belov N. V. *Doklady Akademii Nauk USSR* **183** (1968), [in Russian]

10. Maksimov B. A., Kharitonov Y. A., Ilyhin V. V., Belov N. V. *Kristallographya* **15**, 926 (1970), [in Russian]

11. Becerro A. I., Escudero A. *Phase Transitions* **77**, 1093 (2004)

12. Persson K. *Materials Project* (2014), https://materialsproject.org/mp-3520

13. Probst S., Rotzinger H., Ustinov A. V., Bushev P. A. *Phys. Rev. B* **92**, 014421 (2015)

14. Equall R. W., Cone R. L., Macfarlane R. M. *Phys. Rev. B* **52**, 3963 (1995)

15. Könz F., Sun Y., Thiel C. W., Cone R. L., Equall R. W., Hutchenson R. L., Macfarlane R. M. *Phys. Rev. B* **68**, 085109 (2003).

16. Hee-Jin L., Welinski S., Ferrier A., Goldner P., Morton J. J. L. *Phys. Rev. B* **97**, 064409 (2018)

17. Sugar J., Kaufman V., Spensor N. *J. Res. of NBS* **83**, 233 (1978).

18. Haumesser P.-H., Gaume R., Viana B., Antic-Fidancev E., Vivien D. *J. Phys.: Condens. Matter* **13**, 5427 (2001)

19. Tiranov A., Ortu A., Welinski S., Ferrier A., Goldner P., Gisin N., Afzelius M. *Phys. Rev. B* **98**, 195110 (2018)

20. Kurkin I. N., Chernov K. P. *Physica B* **101**, 233 (1980)

21. Kandrashkin Y. E., Zavartsev Y. D., Koutovoi S. A., Sukhanov A. A. *Applied Magnetic Resonance* **49**, 1313 (2018)

22. Kandrashkin Y. E., Sukhanov A. A., Tarasov V. F. *Applied Magnetic Resonance* **50**, 469 (2019)

23. Sukhanov A. A., Likerov R. F., Eremina R. M., Yatsyk I. V., Gavrilova T. P., Tarasov V., Zavartsev Y. D., Kutovoi S. A. *Journal of Magnetic Resonance* **295**, 12 (2018)

24. Abragam A., Bleaney B. *Electron Paramagnetic Resonance of Transition ions* (Oxford University Press, 1970)

25. Aminov L. K. *Zh. Eksp. Teor. Fiz* **42**, 783 (1962)

26. Mims W. S., Nassau K., McGee J. D. *Phys. Rev. B* **123** (1961)

27. Schweiger A., Jeschke G. *Principles of Pulse Electron Paramagnetic Resonance* (Oxford University Press, 2001)

28. Zhidomirov G. M., Salikhov K. M. *Theoretical and Experimental Chemistry* **4**, 332 (1971)